Available online at www.sciencedirect.com
SCIENCE DIRECT®
Estuarine, Coastal and Shelf Science 63 (2005) 43–56
ESTUARINE COASTAL AND SHELF SCIENCE
www.elsevier.com/locate/ECSS

Sediment transport on the mid-continental shelf in Onslow Bay, North Carolina during Hurricane Isabel

P. Ansley Wren[a,*], Lynn A. Leonard[b]

[a]Texas Institute of Oceanography, Texas A&M University, Galveston, TX 77553, USA
[b]Center for Marine Science, University of North Carolina at Wilmington, Wilmington, NC 28409, USA

Received 13 February 2004; accepted 15 October 2004

Abstract

Hurricane Isabel made landfall on the southeastern U.S. coast along the lower Outer Banks of North Carolina near Cape Lookout, NC on September 18, 2003. An instrumented quadrapod frame moored approximately 43.5 km off the coast of Wilmington, NC in Onslow Bay, at a depth of approximately 30 m, was present on the shelf when the hurricane passed approximately 160 km from Onslow Bay. The attached instrumentation includes a downward-looking Pulse-Coherent Acoustic Doppler Profiler (PC-ADP) and an upward-looking Acoustic Doppler Current Profiler (ADCP). Simultaneous measurements of flow velocities from the surface to the seabed along with acoustic backscatter measurements and seabed elevation were obtained during this storm event. Three days prior to the direct effects of the hurricane, long-period swells (14–17 s) began to impact the area causing sediment transport to occur on the mid-shelf. Shear velocities calculated from a bottom boundary layer model ranged from approximately 6 to 10 cm s^{-1} over the course of the sediment transport event. Based on shear velocity calculations, bedload and suspended sediment transport were occurring at the site 72 h prior to the passage of the hurricane as long-period swells reached heights of 4 m. The seabed altimeter recorded large fluctuations during the storm but was unable to trace elevation changes due to the presence of a highly concentrated layer of suspended sediments in the lower 10 cm of the bottom boundary layer. Large amounts of suspended sediment transport occurred in the along-shelf direction towards the southwest after tropical storm force winds of 30 m s^{-1} began to directly affect the area and wind-driven currents were generated. Wind-driven, subtidal currents responded rapidly to local wind forcing and shifted from 15 cm s^{-1} towards the southwest to 16 cm s^{-1} towards the northeast. Model calculated velocity profiles compared well with measured current velocity profiles. Boxcores collected pre- and post-storm show a storm layer of approximately 5 cm and a sediment trap that was attached to the frame 30 cm above the bed collected approximately 400 cm^3 of fine to medium sands that were suspended during the storm.

Keywords: sediment transport; bottom boundary layer model; cross-shelf transport; Hurricane Isabel

1. Introduction

It is well documented that storm processes dominate sediment transport on many continental shelves (Madsen et al., 1993; Wright et al., 1986, 1994; Li and Amos, 1999; Ogston and Sternberg, 1999; Traykovski et al., 1999; Williams and Rose, 2001; Wiberg et al., 2002). The importance of the role of storms in sediment transport on shelves and the effect of these events on coastal change has become more apparent in recent years. With improvements in instrumentation and technology, more field studies have been initiated and conducted to measure sediment transport processes on

* Corresponding author. Texas Institute of Oceanography, Texas A&M University, PO Box 1675, Galveston, TX 77053, USA.
E-mail address: wrenp@tamug.edu (P.A. Wren).

0272-7714/$ - see front matter © 2004 Elsevier Ltd. All rights reserved.
doi:10.1016/j.ecss.2004.10.018

continental shelves during storms. However, due to the unpredictability of storms and the difficulties and expense in obtaining measurements during these conditions, a paucity of field data exists. Empirical information on near-bottom currents, suspended sediment concentrations, and seabed changes that occur during storm events are needed to verify and further refine existing process-oriented models that can be applied to sediment transport on shelves.

Along the southeastern U.S. east coast, tropical cyclones are a common occurrence during the hurricane season (June 1–November 30). The consequences of these storms can be devastating in some cases, not only because of the destruction of the developed coastline, but also due to the dispersal of offshore infaunal benthic communities which are important in sustaining productive fisheries habitats on the shelf.

2. Study area

Onslow Bay is located off the southeastern coast of North Carolina in the northern region of the South Atlantic Bight (SAB). It is bounded to the northeast by Cape Lookout and to the southwest by Cape Fear, and by the shelf edge and Gulf Stream to the east (Fig. 1). The mean tidal range in Onslow Bay is approximately 1.0 m and is dominated by the M2 component (Pietrafesa et al., 1985). Average significant wave heights are 1.5 m with a dominant period of 8.0 s as measured at the NOAA C-Man station (National Oceanographic Data Center, 2000) (Fig. 1). This ''sediment-starved'' continental shelf is characterized by a complex sequence of rocky outcrops with relief up to 10 m (Renaud et al., 1997) and a thin and discontinuous veneer of Holocene sediment that is generally not accumulating on the shelf. These hardbottom sites in Onslow Bay form the framework for the highly productive ''livebottom communities'' that are important to commercial and recreational fisheries and thus are of major economic importance (Riggs et al., 1998).

3. Methods and instrumentation

As part of the Coastal Ocean Research and Monitoring Program (CORMP) at the University of North Carolina at Wilmington, an instrumented quadrapod frame has been maintained on the mid-continental shelf (33° 59′N, 77° 21′W) in Onslow Bay since April 2000. This instrumentation was present on the shelf when the center of Hurricane Isabel passed approximately 160 km from Onslow Bay and made landfall along the lower Outer Banks of North Carolina near Cape Lookout, NC on September 18, 2003. The instrumented frame is moored 43.5 km off the coast of Wilmington, NC at a depth of approximately 30 m adjacent to a productive marine hardbottom area (Fig. 2). The attached

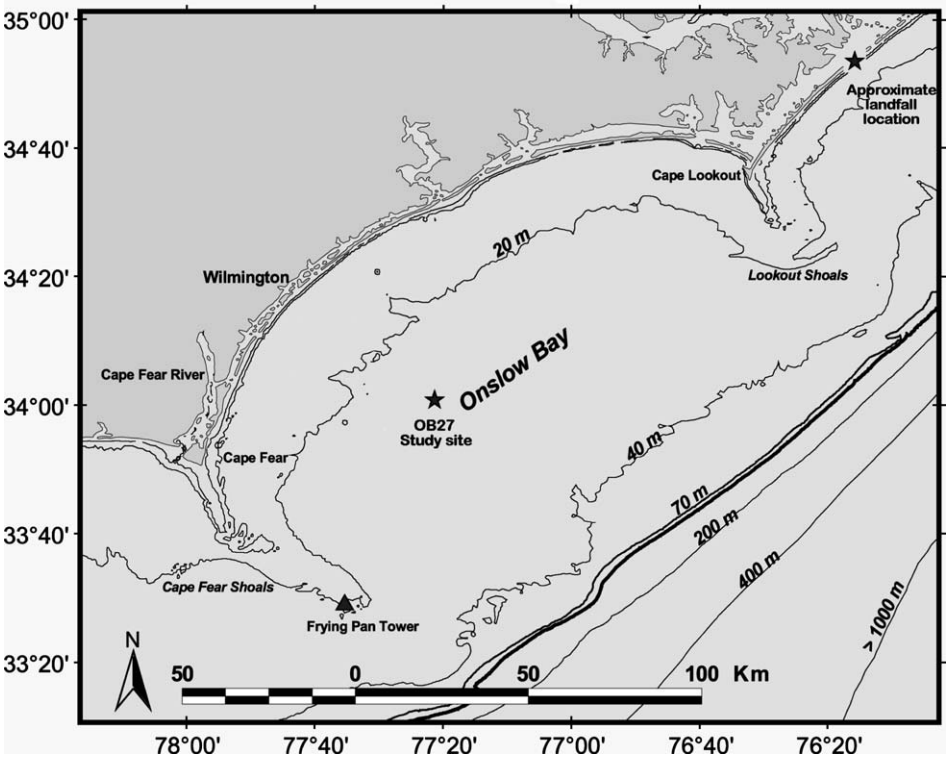

Fig. 1. Onslow Bay is located between Cape Lookout and Cape Fear, NC. OB27 marks the study site, 27 miles off the coast of Wilmington, NC. FPT is the location of the NOAA C-man station where wind and wave data were collected. Hurricane Isabel made landfall northeast of the study site.

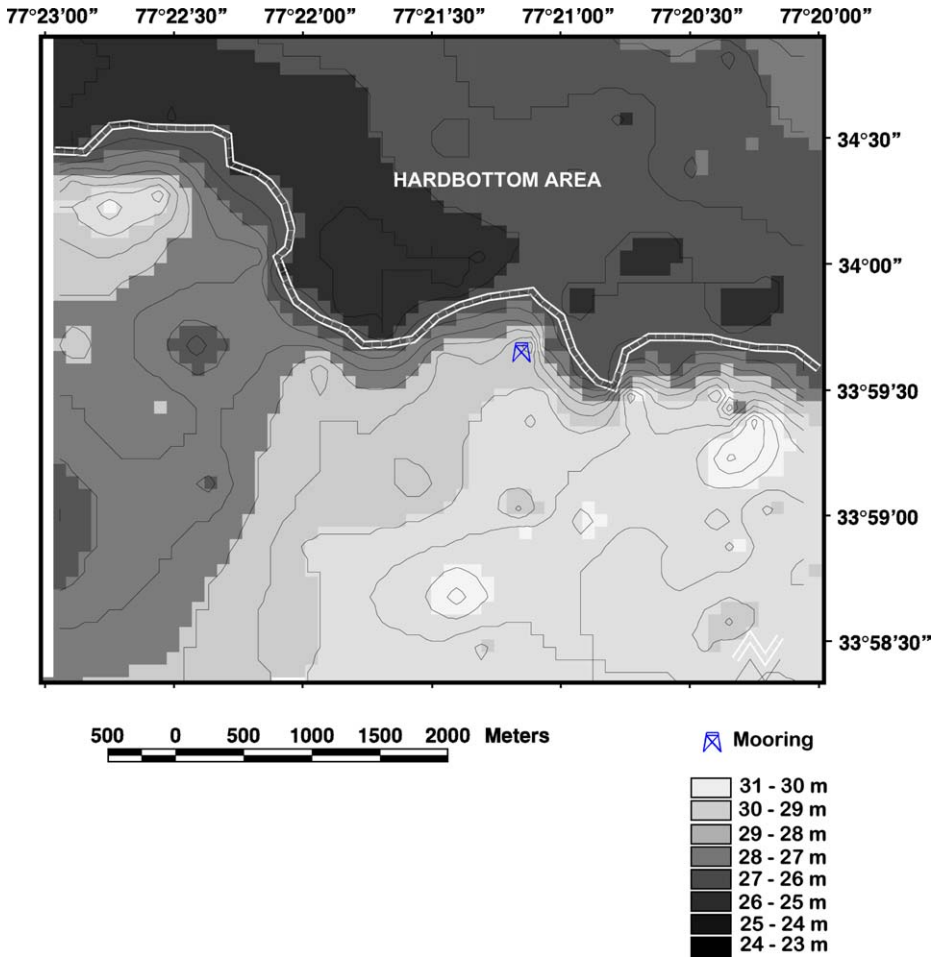

Fig. 2. Contour plot showing the bathymetry of the study area and the extent of hardbottom area located north and east of the study site. The white lines indicate the reef ledge (Head, 2004).

instrumentation includes a downward-looking Pulse-Coherent Acoustic Doppler Profiler (PC-ADP) and an upward-looking Acoustic Doppler Current Profiler (ADCP). Simultaneous measurements of flow velocities from the surface to the seabed along with acoustic backscatter measurements and seabed elevation were obtained during this storm event and are reported here. A bottom boundary layer (bbl) model (Styles and Glenn, 2000, 2002) was used to calculate bed shear stresses due to wave–current interactions during the event. The bbl model also generated near-bottom current, suspended sediment concentration and transport profiles. Current profiles were compared to the high-resolution current profiles measured in the lower boundary layer, and the bbl model was used to quantify the sediment transport that occurred during the event.

In order to examine atmospheric forcing over the duration of the storm, available wind and wave data were used from a nearby National Data Buoy Center (NDBC) meteorological station. The meteorological station, FPSN7, is located on Frying Pan Shoals at the southern boundary of Onslow Bay approximately 61 km southwest of the study site (Fig. 1). Wave heights reported in this paper are root-mean-squared (r.m.s.) values.

The downward-looking 1.5-MHz PC-ADP is secured approximately 150 cm above the seabed and measures velocity profiles of the bottom boundary layer in 10-cm bins. The instrument samples in "burst mode" at 2 Hz for 10 min every 2 h. When examining bottom boundary layer conditions and calculating the bed shear stresses, the burst-averaged velocity time series at 1 mab was used. The ADCP is situated approximately 2 m above the seabed in an upward-looking configuration. The instrument is a 600-kHz RDI Workhorse Sentinel that profiles the overlying water column in 1-m bins at 1 Hz and averages the data over a 60-s averaging interval. The ADCP records a velocity profile of the upper water column once every 5 min. For all current velocity data, the along-shelf axis is taken at 55.6° east of north following Pietrafesa et al. (1994) and is positive towards the southwest; the positive across-shelf direction is directed offshore.

The PC-ADP also measures temperature and pressure, and serves as a bottom altimeter to monitor changes in seabed elevation. The three acoustic beams in the downward-looking transducer detect where the seabed is

located under the frame once during each 10-min burst and these data are used to determine changes in seabed elevation throughout the event. To measure relative changes in turbidity, the 1.5 MHz PC-ADP acoustic backscatter signal (ABS) was used. This approach is useful for approximating relative changes in suspended particulate in the water column, and is similar to the Acoustic Backscatter Sensor which has been shown to be especially successful with sands in sediment transport studies in the U.S. and the U.K. (Traykovski et al., 1999; Battisto, 2000; Williams and Rose, 2001).

Seabed altimetry and pre- and post-storm diver-collected boxcores extending approximately 18 cm into the seabed were used to examine the depth of sediment reworking following storm disturbance. Following collection, the boxcores were sub-sampled at 5-cm intervals. Pre- and post-event stratigraphy was examined to identify distinct storm deposits and the depth of reworking due to physical processes and post-event bioturbation. In addition, a sediment trap was attached to the frame approximately 30 cm above the bottom that collected suspended sediments in the water column during the storm. The grain-size distributions of the boxcore sub-samples and the material collected in the sediment trap were determined using a Beckmann-Coulter LS 200 particle sizer.

The input data required for the bbl model during the event included: (1) PC-ADP burst-averaged mean current (U_r) measured at a 1 mab reference elevation (Z_r) in the bottom boundary layer; (2) near-bottom orbital velocities (U_b) and near-bottom wave excursion amplitudes (A_b); and (3) the wave and current incidence angle (Φ_{cw}). Bottom r.m.s. wave velocities, u_b, were determined using the instantaneous velocity record, $u(t)$, for each burst after the mean current, $\vec{u}_c$, had been removed. Following Madsen (1995), the variance for each horizontal direction was determined and the near-bottom orbital velocity amplitude of the equivalent periodic wave was taken as:

$$u_b^2 = 2\left(\sigma_u^2 + \sigma_v^2\right)$$

Wave direction was calculated as the direction of maximum variance for each burst:

$$\theta = \frac{1}{2}\tan^{-1}\left(\frac{2\sigma_{uv}^2}{\sigma_{uu}^2 - \sigma_{vv}^2}\right)$$

where θ = direction (rad), σ_{uu}^2 and σ_{vv}^2 = variances of the respective eastward and northward velocity components (u and v), and σ_{uv}^2 = covariance of the velocities. Wave periods from two ADCPs located on the inner shelf in Onslow Bay and the NDBC station showed excellent agreement; therefore, wave periods (T_{dom}) from the NDBC meteorological station were input into the bbl model.

Table 1
Sediment grain-size distribution model inputs (percent per fraction)

Sediment diameter (cm)	0.004	0.0106	0.0269	0.06842
Percent	1.0	37.3	51.5	10.2

The bottom shear stresses due to wave–current interactions were determined using the bbl model, and subsequently, the suspended sediment transport and bedload transport rates could be determined. The suspended sediment concentration and transport profiles were generated using four different grain-size fractions, each with the percentage that was found in surface samples from the site (Table 1). The total suspended sediment transport rate was determined from the following:

$$\vec{Q} = \sum_{i=1}^{n} \vec{q}_{bi} f_i$$

where f_i is the percentage of material of size i available on the seabed and n is the number of grain sizes used. The bedload transport rates were calculated using a modified version of the Meyer-Peter and Muller (1948) equation for oscillatory flows that utilized instantaneous wave velocities (Madsen and Wikramanayke, 1991). Bedload flux was calculated as:

$$Q_B = 8\left(\left|\theta_w^{sf}\right| - \theta_{cr}\right)^{1.5} \frac{\theta_w^{sf}}{\left|\theta_w^{sf}\right|} \rho_s d\sqrt{(s-1)gd} \quad \text{if} \quad \left|\theta_w^{sf}\right| > \theta_{cr}$$

$$Q_B = 0 \quad \text{if} \quad \left|\theta_w^{sf}\right| < \theta_{cr}$$

and Q_B = bedload flux in g cm^{-1} s^{-1}, θ_w^{sf} = instantaneous skin friction Shield's parameter due to wave velocities, θ_{cr} = critical Shield's parameter, s = specific gravity of the sediment grains, g = acceleration due to gravity, and d = the median grain-size diameter of the sediment (cm). It has been shown by Traykovski et al. (1999) that for the purposes of predicting initiation of sediment motion, it is often sufficient to consider only wave stresses when the shear stresses due to waves are much greater than the shear stresses due to currents. The mean ratio of τ_c^{sf}/τ_w^{sf} for the entire event was 0.038, with a maximum value of 0.2; therefore, only the instantaneous wave velocities were used to calculate the bedload flux. The instantaneous skin friction Shield's parameter due to wave velocities was calculated following Nielsen (1992):

$$\theta_w^{sf}(t) = \frac{1}{2}\frac{f_{2.5}\sqrt{2}u_b u_w(t)}{gd(s-1)}$$

where $f_{2.5}$ = the wave friction factor developed by Swart (1974), where the grain roughness is defined by 2.5 times the median grain diameter, and where $u_w(t) = u(t) - \vec{u}_c$.

The bbl model also predicted ripple geometry which was compared to the measured seabed altimetry data throughout the event. This study is unique given that diver observations, boxcores, and sediment samples were collected at the mid-shelf site as the hurricane began to impact the area, as well as immediately after hurricane passage. These types of data and observations were critically important in correctly interpreting the instrumentation measurements and the bbl model output.

4. Results

4.1. The hurricane

Isabel developed into a tropical storm on September 6, 2003 in the central Atlantic Ocean. Within 48 hours, Tropical Storm Isabel was a major category 3 hurricane on the Saffir–Simpson scale. Isabel reached category 5 strength on 11 September with maximum winds above 248.4 km hr^{-1}. Over the next four days Isabel's intensity fluctuated, maintaining winds of 241.2 km hr^{-1} or greater, with maximum sustained winds reaching 257 km hr^{-1} and gusts to 313.2 km hr^{-1}. By 15 September, Isabel was north of the Dominican Republic at approximately 25.0° N and 70.0° W and began a northwesterly turn towards the southeastern U.S. coast. The hurricane started to weaken in intensity as it traveled north and approached the southeastern U.S. coast, and was a category 2 hurricane when it made landfall in the southern Outer Banks of North Carolina at approximately 1600 UTC on 18 September.

4.2. Wind and wave forcing

Long-period swells (14–17 s) preceded the hurricane and wave heights increased steadily (Fig. 3) as the hurricane traveled closer to the site from 15 September through mid-day on 18 September. On 15 September, three days prior to landfall, winds were from the north and less than 10 m s^{-1} in the study area. Early on the 16 September local winds became NNE, and wave heights at the NDBC meteorological station built to 3 m as wave periods decreased slightly (Fig. 3). Over the next 24 h, wave conditions consisted of a combination of hurricane swells and locally generated seas. Northerly winds increased to 15–20 m s^{-1} on the 17th while wave heights were 2.5–3.75 m and dominant wave periods ranged from 14 to 17 s (Fig. 3). Winds slightly greater than 20 m s^{-1} remained from the north, until early on the 18th when they began to gradually shift from

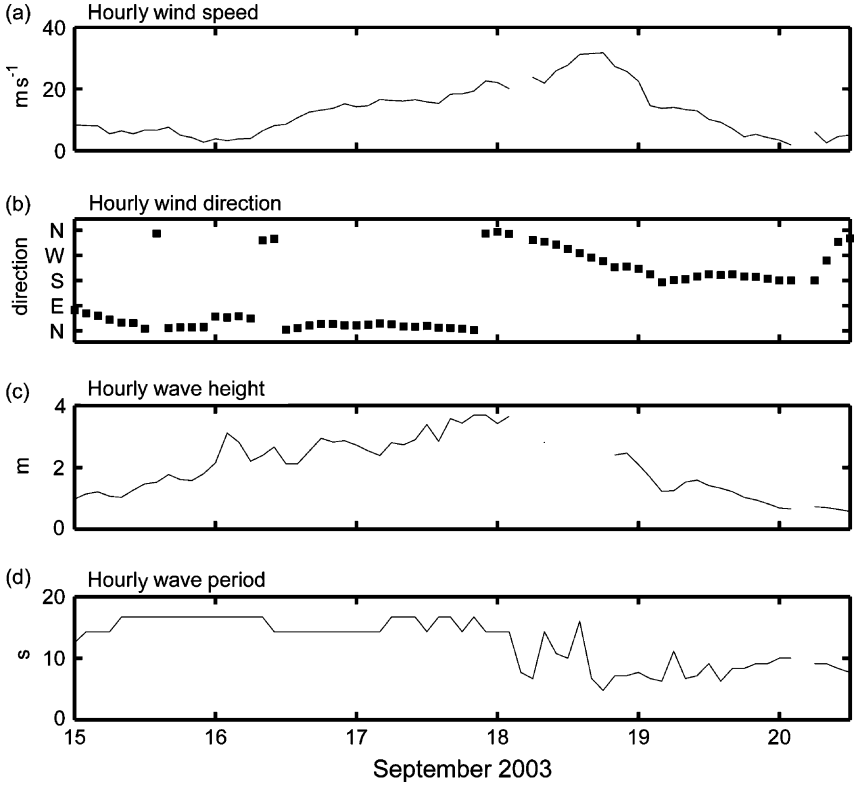

Fig. 3. Hourly wind and wave data at the NOAA Frying Pan Tower C-Man station (http://www.ndbc.noaa.gov/FSN7) during Hurricane Isabel. The wave gauge failed during the peak storm conditions on September 18 and wave periods were determined from the spectra of the individual velocity records from each burst.

northerly to westerly and increased to over 30 m s^{-1}. The wave gauge failed at this time, although based on the increase in wind speed and the bottom velocities measured by the PC-ADP, it is evident that wave heights increased during this period. By 1400 UTC on the 18th, winds were from the west at 31 m s^{-1}. These conditions were sustained for 2 h and comprised the maximum wind velocities measured in the study area during the passage of the hurricane. Winds continued to back around to a southwesterly and then southerly direction over the next 8 h and decreased to 15 m s^{-1}. Wave heights in the area decreased late on the 18th as the hurricane passed to the north and northeast of Onslow Bay and made landfall. Southerly winds persisted for the next 24 h and wave heights further decreased to less than 1 m with wave periods of 8–10 s by mid-day on the 19th. Overall, the wave impacts of Hurricane Isabel were felt at the site for approximately 4.5 days.

4.3. Bottom boundary layer dynamics

4.3.1. September 15

The initial influence of Hurricane Isabel was associated with the long-period swells that propagated from the storm and began to impact the study area on 15 September, three days prior to landfall. These longer period swells caused bottom wave orbital velocities to increase to 20–40 cm s^{-1} on 15 September (Fig. 4). Mean currents at this time were tidally dominated and less than 10 cm s^{-1} at 1 mab and 15 cm s^{-1} at 4 mab (Fig. 5). Shear velocities calculated from the bbl model increased from approximately 5.5 cm s^{-1} to 6.8 cm s^{-1} over the course of the day (Fig. 4).

Model calculated current profiles generated at 1000 UTC were in very good agreement with the measured current profile at this time, and showed weak flow speeds less than 5 cm s^{-1} in the bottom boundary layer (Fig. 7a). The concentration profile output from the bbl model at this time indicates that a small amount of sediment was being actively suspended in the lowest part of the bottom boundary layer due to wave action. This is corroborated by the ABS data showing elevated readings at 10 cmab (Fig. 4d). The suspended sediment transport profile produced by the bbl model suggests that only a small amount of transport occurred at this time due to a combination of weak currents and relatively low concentrations of suspended sediments in the bottom boundary layer (Fig. 7a). When using the calculated shear

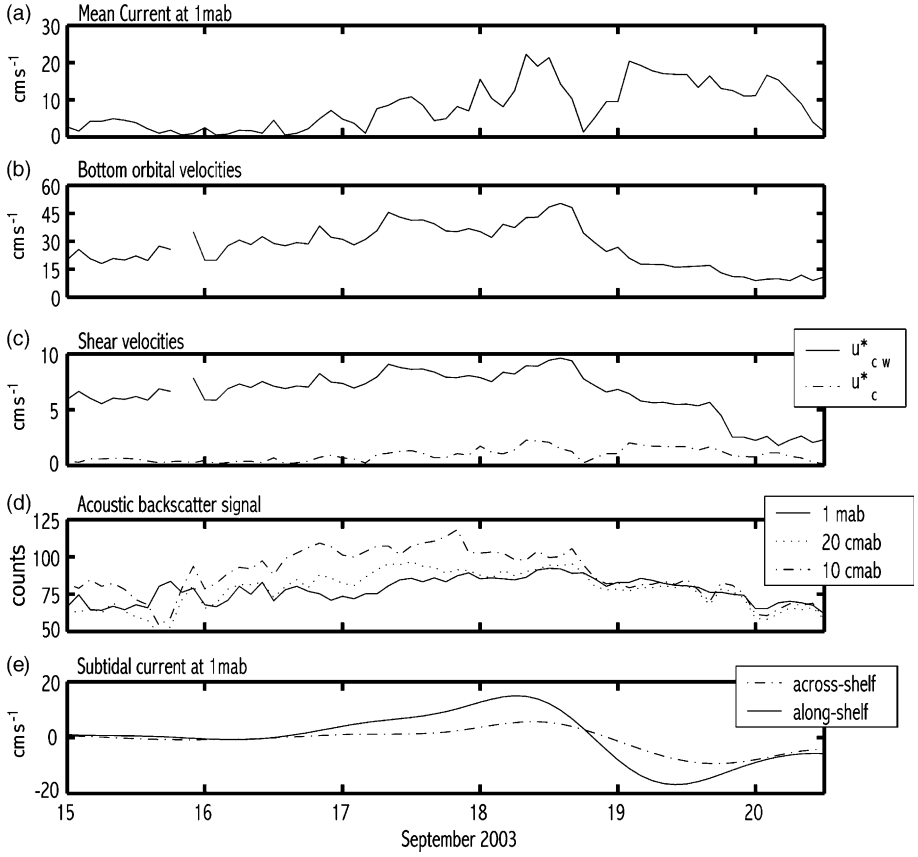

Fig. 4. Hurricane Isabel: (a) mean current speed at 1 mab; (b) bottom orbital velocities; (c) combined wave–current and current shear velocities; (d) acoustic backscatter signal; (e) along- and across-shelf subtidal currents. The acoustic backscatter signal was used as a proxy for determining relative changes in suspended sediment concentration at different heights above the bed. The positive along-shelf direction is towards the southwest, and the positive across-shelf direction is offshore.

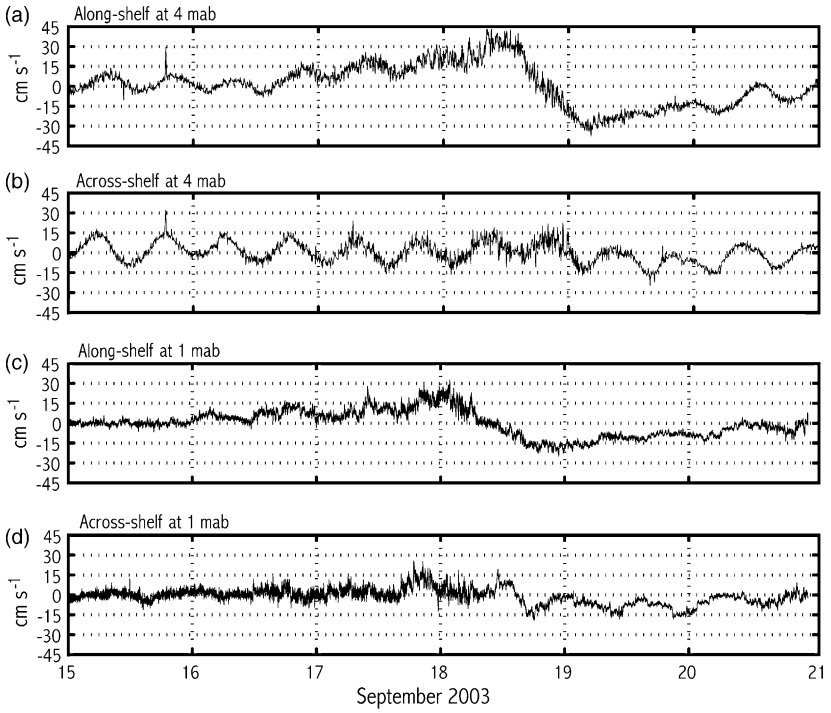

Fig. 5. The top two panels show the Acoustic Doppler Current Profiler current velocities at 4 mab in the (a) along-shelf and (b) across-shelf direction. The bottom two panels show the burst-averaged current velocities from the Pulse-Coherent Acoustic Doppler Profiler at 1 mab in the (c) along-shelf and (d) across-shelf direction. The positive along-shelf direction is towards the southwest and the positive across-shelf direction is directed offshore in the southeasterly direction.

velocities and grain-size characteristics of bottom sediments at the site, only fine sands with grain diameters of less than 0.0225 cm are predicted to have been in suspension at this time, based on the condition for full suspension where $w_s/ku_{*m} \approx 1$ (Wiberg and Harris, 1994). The sands that remained on the seabed were transported via bedload transport, however, currents were very weak at this time and the only driving force for transport would have been the asymmetries of the bottom wave velocities. Because the dominant direction of the swells were from the across-shelf direction, skewness was calculated using the across-shelf wave velocities following Traykovski et al. (1999) where $s = \overline{(u(t)^3)}/u_{r.m.s.}$ (Fig. 6). The skewness values indicate that asymmetries fluctuated between onshore and offshore, and do not suggest a dominant direction. Bedload rates were calculated from the instantaneous wave velocities and reflect this pattern of skewness. Bedload transport flux occurred at rates of 0.0050 g cm^{-1} s^{-1}, alternating between the onshore and offshore directions (Fig. 8).

Model calculated ripple heights at this time were predicted to be approximately 4–5 cm, with a steepness of approximately 0.10 (Fig. 8a, b). The bbl model ripple geometry calculations are also consistent with the seabed elevation data recorded at this time (Fig. 8c), which show fluctuations of 1–2 cm suggesting the presence of ripples, and with anecdotal reports from divers of ripples of approximately 4 cm in height present on the seabed.

4.3.2. September 16

Sediment transport processes continued to intensify over the next 24 h. At approximately 1000 UTC, the dominant wave period decreased to 14 s, as northerly winds began to increase and wave conditions changed from swell-dominant to a combination of locally generated waves and hurricane swell. The bottom orbital velocities associated with these waves ranged

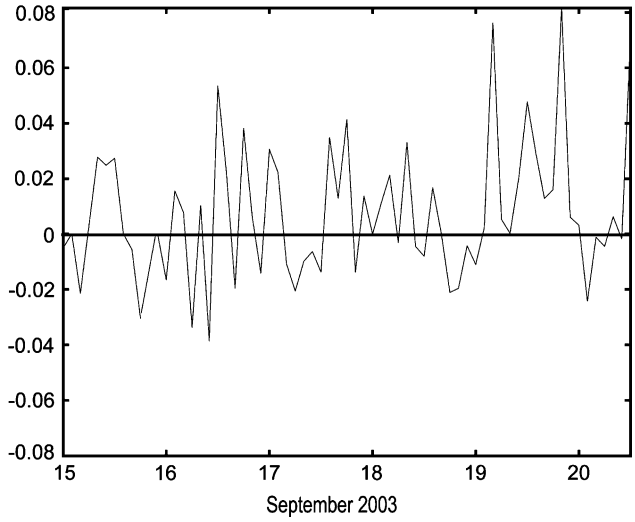

Fig. 6. Wave skewness of the across-shelf component of orbital velocity for each burst throughout the passage of Hurricane Isabel.

from 18 to 38 cm s^{-1} throughout the day (Fig. 4). Mean currents continued to be tidally dominated and weak (< 5 cm s^{-1} at 1 mab) in the bottom boundary layer. However, by 2000 UTC a weak subtidal current had been generated in the along-shore direction due to the increase in sustained northerly winds, which had increased to 15 m s^{-1}.

Wave–current shear velocities increased to approximately 7.5 cm s^{-1} towards the end of the day and created conditions for full suspension based on the median grain diameter of sediment at the site. Model calculated current profiles at 2200 UTC generally agree with the measured current profiles and indicate that mean currents continued to be weak in the bottom boundary layer (Fig. 7b). Although suspended sediment concentrations and transport had increased, the transport was limited due to the weak current that was present (Fig. 7b). A weak along-shelf subtidal current of less than 5 cm s^{-1} existed at this time (Fig. 4) and it was this current that steered the direction of suspended sediment transport. In addition, across-shelf bedload transport was still occurring at the site in association with the long-period swells that were propagating across the shelf. Calculated bedload flux increased to

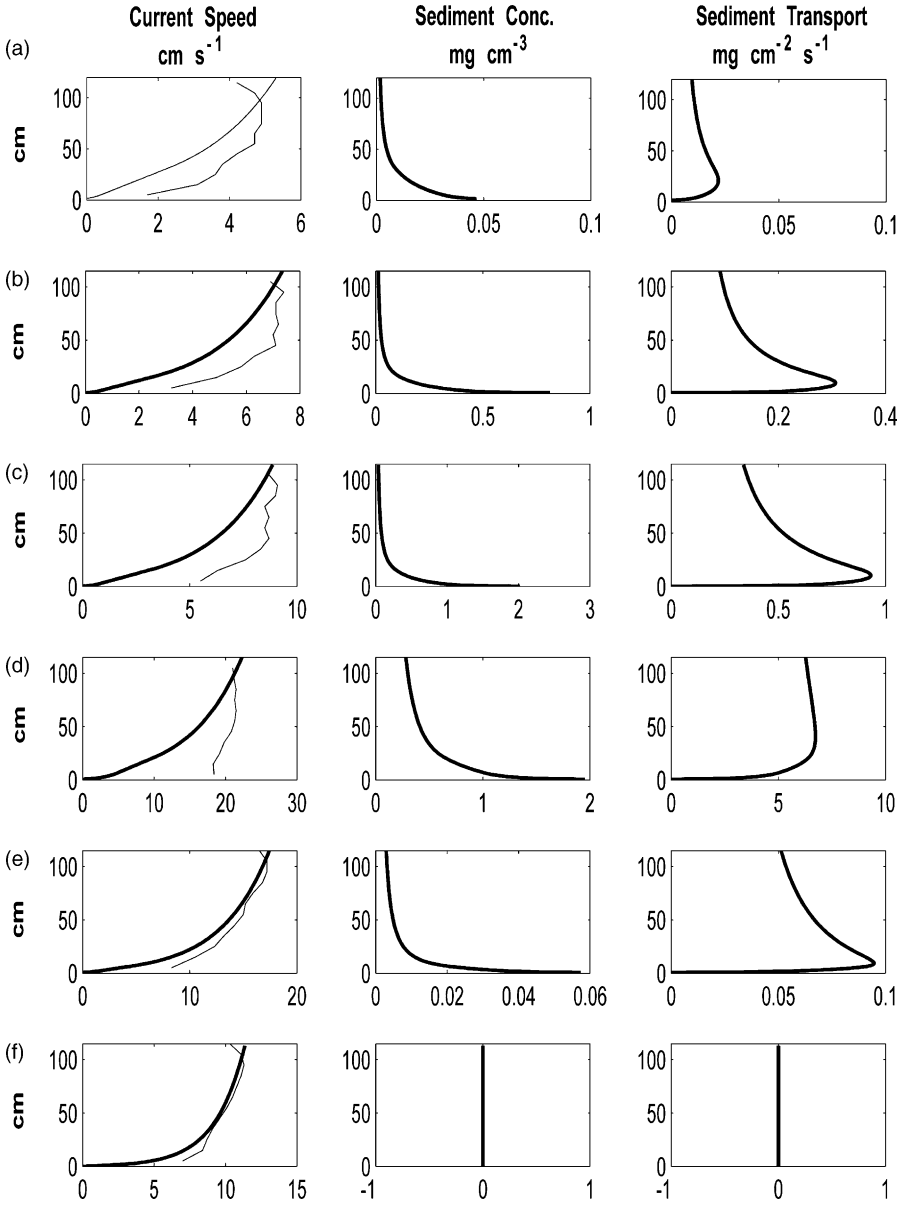

Fig. 7. Bottom boundary layer model output for six bursts throughout the passage of Hurricane Isabel. Modeled current profiles were compared to the burst-averaged measured currents in the bottom boundary layer where the bold line indicates bbl model output. (a) 15 September – swells began to impact the site; (b) 2200 UTC 16 September – weak currents hinder sediment transport; (c) 1400 UTC 17 September – sediment transport increases; (d) 1400 UTC 18 September – peak wind conditions; (e) 1200 UTC 19 September – waning of storm event; (f) 1200 UTC 20 September – sediment transport comes to an end.

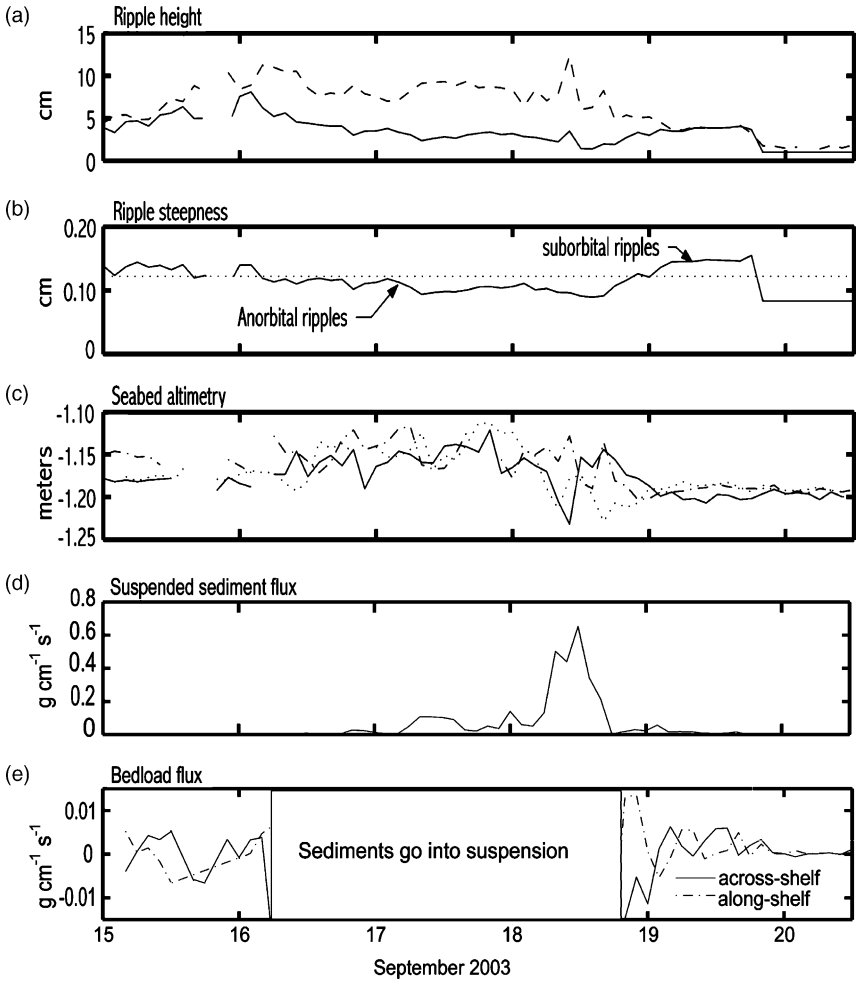

Fig. 8. Hurricane Isabel: model calculated (a) ripple heights and wave boundary layer thickness; (b) ripple steepness; (c) measured seabed altimetry data from each of the three beams; (d) model generated depth-integrated suspended sediment flux; (e) Meyer-Peter–Muller bedload flux incorporating velocity skewness. Full suspension occurred when the skin friction shear velocity exceeded the critical shear velocity for full suspension early on the 16th and continued throughout the event until late on the 18th. Suspended sediment flux was an order of magnitude larger than bedload flux for fine sands at the mid-shelf site.

$0.015\ g\,cm^{-1}\,s^{-1}$ before the fine sands went into suspension (Fig. 8e). The critical velocity for full suspension for the median grain size was exceeded at this time; therefore shear velocities increased throughout the day; therefore, suspended sediment transport was the dominant mode of transport from the 16th until the waning of the storm on the 19th (Fig. 8d, e).

The bbl model predicted that low amplitude anorbital ripples would have been present at this time which would have consisted of sands with grain-size diameters of greater than 0.0300 cm, while sediments finer than 0.0300 cm would have been in full suspension. These results are consistent with the empirical formulations of Wiberg and Harris (1994) that suggest the formation of anorbital ripples under conditions comparable to the observed bottom orbital velocities at this time and the median grain-size diameter. Anorbital ripples are the most common ripples that occur in shelf environments and have steepness values of 0.12 or less, which decrease with increasing wave energy. The seabed elevation measured by the 3 PC-ADP beams all show fluctuations of 2–5 cm with an increase in height over the course of the day (Fig. 8c). There is, however, a discrepancy here between the model and the measured data. The model shows ripple height and steepness decreasing throughout the day; exhibiting heights of approximately 3 cm with steepness values of only 0.10 (Fig. 8a, b). This discrepancy between the seabed altimetry data and the bbl model ripple geometry calculations is addressed further in the following section.

4.3.3. September 17

As the storm continued to approach the site, bottom orbital velocities and current velocities continued to increase (Fig. 4). Northerly winds increased in magnitude from $16\ m\,s^{-1}$ to $22\ m\,s^{-1}$ (Fig. 3) and bottom orbital velocities continued to increase, reaching $45\ cm\,s^{-1}$ (Fig. 4b). Wave–current shear velocities

increased throughout the day and ranged from 7.0 to 8.5 cm s^{-1} (Fig. 4c). The acoustic backscatter signal increased to approximately 80 counts at 1 mab and was even greater in the lower 10 cm (Fig. 4d). The bbl model concentration profile at 1400 UTC agrees well with the ABS data and indicates that suspended sediment concentrations had increased due to the increase in wave energy (Figs. 3c, 4b, 8a). The along-shelf wind-driven current at 1 mab reached a maximum of 12 cm s^{-1} late in the day and was significantly stronger than the across-shelf current that began to develop mid-day on 17 September (Fig. 4e). The measured and modeled current profiles both show an increase in mean current speed throughout the bottom boundary layer compared to the previous day (Fig. 7c). The suspended sediment transport profile provided by the model indicates that transport was occurring at rates of 0.5–0.9 mg cm^{-2} s^{-1} throughout the bottom boundary layer with the highest transport rates in the lower 20 cmab (Fig. 7c). Calculations indicate that sand with a grain size less than or equal to 0.0355 cm would have been in full suspension under these conditions.

The bbl model ripple calculations show ripple heights continuing to decrease with ripple heights of 3 cm and low steepness values of 0.9–1.0. The seabed altimetry data are, however, inconsistent with these measurements and show large fluctuations of 2–5 cm throughout the day, as well as an increase in seabed elevation. Again, this discrepancy is discussed in further detail in the following section of the manuscript.

4.3.4. September 18 and 19

As the hurricane made its closest approach to the study site on 18 September, winds increased creating wind-driven currents throughout the water column while bottom orbital velocities remained high. The along-shelf mean currents at 4 mab and 1 mab were dominated by the wind-driven response, and the semi-diurnal tidal signal was only apparent in the across-shelf flows (Fig. 5). Early on 18 September, when winds were from the north at 20 cm s^{-1}, along-shelf southwesterly currents reached over 30 cm s^{-1} at 4 mab and 15 cm s^{-1} at 1 mab. As the storm passed by the site between 0400 UTC and 1000 UTC, wind direction backed around from northerly to westerly (Fig. 3), however, the subtidal flow continued to be southwesterly and reached a maximum of 15 cm s^{-1} while an offshore wind-driven flow of 5 cm s^{-1} was generated (Figs. 3, 4). The maximum hourly wind speed for this event occurred at 1400 UTC and was from the west-southwest sustained at 31 m s^{-1} (Fig. 3). During maximum wind conditions, the wind-driven along- and across-shelf currents were 10 cm s^{-1} and 5 cm s^{-1}, respectively. Wave periods decreased to 6–10 s and bottom orbital velocities were slightly greater than 50 cm s^{-1}, while wave–current shear velocities reached 9.6 cm s^{-1} at 1400 UTC (Fig. 4). The model generated suspended sediment concentrations were between 0.5 and 2 mg cm^{-3} throughout the bottom boundary layer at this time and indicate that sediments were becoming well-mixed throughout the bottom boundary layer. The ABS measurements corroborate these results and show a convergence in the signal amplitude at all levels above the bed. The maximum suspended sediment transport rates occurred at this time and were approximately 7 mg cm^{-2} s^{-1} throughout the bottom 1.2 m (Fig. 7d). This was due to the concurrent increase in both suspended sediment concentration and wind-driven current speed during peak storm conditions.

The seabed altimetry data show large fluctuations of 10 cm during this time, while the bbl model predicts that ripples are continuing to decrease in height and steepness. The calculated shear velocities during these peak storm conditions were large enough that ripples should have been approaching wash out conditions, which is consistent with the model output. The grain-size analysis of sediments retained in the sediment trap placed 30 cm above the bed suggests that shear velocities did exceed the critical threshold required for full suspension for all grain sizes finer than 0.0663 cm found at the site.

The peak bottom conditions lasted for only a few hours, as the wind continued to back around to a southwesterly direction and subtidal currents responded very rapidly (Fig. 4). Bottom orbital velocities had decreased to 25 cm s^{-1} by late in the day and shear velocities were 6 cm s^{-1}, thus reducing the resuspension of bottom sediments that occurred over the previous two days. As sediments began to fall out of suspension, bedload transport flux was in the onshore direction and towards the northeast for a brief time occurring at rates of 0.015 g cm^{-1} s^{-1} (Fig. 8e).

The wind direction remained from the southwest over the next 24 h. Early on 19 September, northeasterly along-shelf currents reached 30 cm s^{-1} at 4 mab and 15 cm s^{-1} at 1 mab (Fig. 5) as wave orbital velocities decreased. By 1200 UTC on 19 September, wave orbital velocities were only 15 cm s^{-1}, although the wind-driven, subtidal currents had reached a maximum of 9 cm s^{-1} in the onshore direction and 16 cm s^{-1} towards the northeast. The bbl model current profile for this time agrees very well with the measured current profile (Fig. 7e). Both current profiles indicate an increase in magnitude when compared to earlier bursts and the logarithmic curves of the profiles are very similar throughout the bottom boundary layer. The concentration profile indicates that little sediment was being actively resuspended given the grain-size distribution input into the model. Based on the estimated shear stresses at this time, only the finest fractions of the grain-size distribution would have been actively suspended. The low suspended sediment concentrations predicted by the model were subsequently used to calculate

suspended sediment transport, yielding rates of less than 0.05–0.09 mg cm^{-2} s^{-1} (Fig. 7e). The ABS time series measurements from late on 18 September (Fig. 4) suggest a rapid decrease in sediment concentration at all levels above the bed followed by a gradual decrease on 19 September, as sediment concentrations continued to be homogenous throughout the bottom boundary layer. These data most likely reflect the settling of the coarser fraction, greater than approximately 0.0300 cm, and the retention of the finer fraction in suspension due to skin friction bottom stresses remaining in excess of the critical bottom stress throughout most of the day. Subtidal currents remained strong towards the north-northeast at 1 mab (Fig. 4) and these currents facilitated the advection of the fine sediments retained in suspension.

Seabed altimetry data collected on 19 September show lower seabed elevations from pre-storm data with fluctuations of approximately 1 cm. Under the given wave and current conditions, however, the bbl model predicted the formation of 5 cm ripples on the seabed with steepness values of 0.15, which would be classified as suborbital ripples according to Wiberg and Harris (1994). However, due to the substantial decrease in shear stress on the 19th, bedload flux remained low at approximately 0.005 g cm^{-1} s^{-1} in the offshore direction (Fig. 8).

4.3.5. September 20

On 20 September the sediment transport associated with Hurricane Isabel began to come to an end. Wind-driven, subtidal flows in the bottom boundary layer diminished on 20 September (Fig. 4). Bottom wave orbital velocities were 10 cm s^{-1} and combined wave–current shear velocities remained approximately 2–2.5 cm s^{-1} (Fig. 4). At 0000 UTC, the bbl model indicates that currents had decreased and that the sediment transport event was over (Fig. 7f). This is consistent with the ABS measurements which indicate that suspended sediment levels had decreased to pre-storm levels at all measured heights above the bed (Fig. 4). Fluctuations in the seabed altimetry data diminished on the 20th and these data are in agreement with the bbl model output, which returned to the default model input values for ripple heights.

5. Discussion

5.1. Sediment transport

The two most important contributing factors to the sediment transport that occurred at the mid-shelf site during the hurricane were long-period swells and subtidal flows. As the hurricane swells propagated across the shelf, critical shear velocities for sediment movement were exceeded causing sediment transport to occur three days prior to the storm passage. The bedload transport that occurred on the 15th was associated with long, two-dimensional, narrow-crested ripples with broad troughs that were observed by divers at three locations across the shelf. The seabed altimetry data and the bbl model output also suggest presence of ripples on the seabed on 15 September (Fig. 8). The physical data suggest that these ripples were formed under weak currents and high wave orbital velocities at the seafloor when waves continued to be from the southeast and varied less than 20° from directly onshore. According to Traykovski et al. (1999), when waves are the dominant mechanism for bedload transport associated with ripple migration, wave asymmetries play a critical role. Therefore, on the 15th when suborbital ripples were predicted to be present, the estimated bedload transport associated with the migration of these ripples would have been in the offshore direction due to stronger offshore velocities that occurred throughout the wave cycle of the long-period swells. Bedload transport, however, does not appear to have played a large role in the overall sediment transport during this event as the fine sands at the site started to go into suspension on the 16th and ripples were predicted to decrease in steepness as they transitioned to anorbital ripples. These results are consistent with the ABS data and the concentration profile produced by the bbl model on the 16th, where both indicate increasing amounts of suspended sediment. In addition, when sediments began to fall out of suspension during the waning of the event, shear velocities decreased rapidly and bedload flux remained low. Therefore, due to the low critical shear stresses required for resuspension of the grain sizes found at the mid-shelf site, suspended sediment transport appears to have played a far more dominating role in the transport of the fine sands during this event. Although not directly examined during this study, our results also suggest that nearby coarse grained patches of sediment located near the hardbottom would have been transported as bedload during the periods of higher critical shear velocities documented near peak storm conditions.

As the sediments at the site began to go into full suspension, a subtidal current began to develop in the bottom boundary layer late on 16 September. These quasi-steady, low-frequency currents are capable of transporting sediments that are suspended and mixed into the current boundary layer long distances. The southwesterly subtidal currents coincided with the time of high bottom orbital velocities at approximately 1400 UTC on 18 September. The bbl model output predicted that a significantly larger amount of suspended sediment transport occurred at this time than any other time throughout the event. During these peak conditions, transport was predominantly towards the southwest in the lower 1.2 m of the water column. Maximum

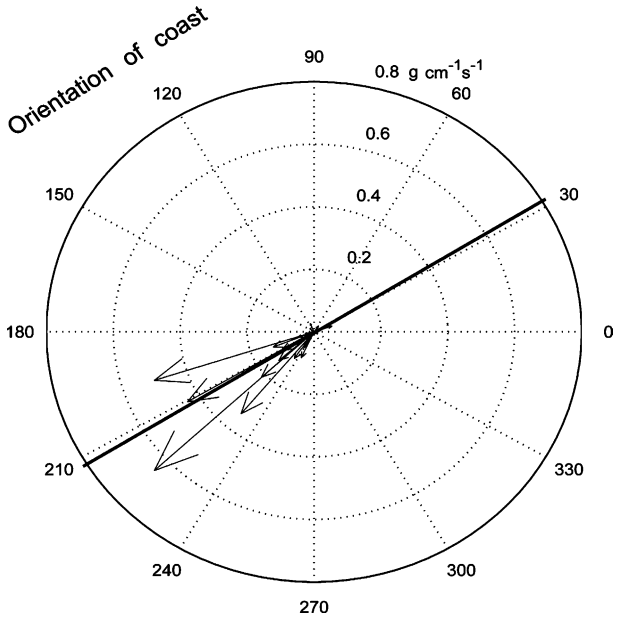

Fig. 9. Compass plot showing the direction of the depth-integrated suspended sediment transport profiles throughout the passage of Hurricane Isabel. Net suspended sediment transport was dominantly in the along-shelf direction.

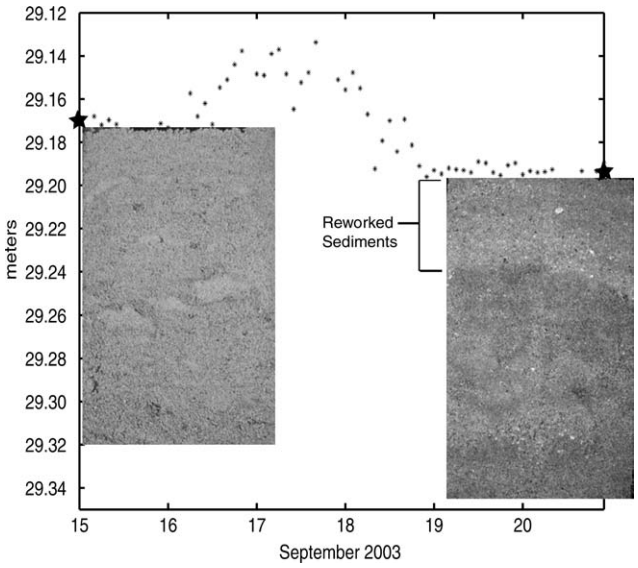

Fig. 10. Pre- and post-boxcores are aligned with the seabed elevation data. The storm layer is visible in the post-storm core as oxidized sediment. There was approximately 2 cm of net erosion of the seabed following storm passage although at least 7 cm of reworking is indicated given the deposition of a 5–6-cm-thick storm deposit.

suspended sediment transport rates were driven by the large bottom shear stresses in combination with strong southwesterly subtidal currents of 15 cm s^{-1} at this time. This dominant southwesterly transport direction is evident in the compass plot showing the direction of all of the vertically integrated suspended sediment transport profiles for each burst throughout the event (Fig. 9). However, near-bottom subtidal currents responded rapidly and were well-correlated ($R = 0.68$) with local wind forcing, changing in magnitude and direction when winds shifted from northerly to southerly late on 18 September. The transport direction subsequently switched toward the northeast, although bottom stresses and suspended sediment concentrations had decreased by this time. Therefore, conditions were less ideal for suspended sediments to be transported in the opposing direction, even though subtidal currents of 16 cm s^{-1} were present. Due to the dominant southwesterly direction of transport, coupled with the limited source of suspended sediment on the extensive hardbottom northeast of the site (Fig. 2), a sediment deficit would have existed at the site. The high ABS signal that was measured at this time most likely resulted from the suspension of locally eroded sediments at the site.

5.2. Seabed altimetry and boxcores

The seabed altimetry data indicate that the post-storm seabed elevation was approximately 2 cm lower than the pre-storm elevation (Fig. 10). The altimetry data also show an approximate 5 cm increase in seabed elevation during the highest energy conditions of the storm. Together, the complete seabed altimetry time series suggests a period of net accretion and bedform development followed by erosion that subsequently removed this material. This conceptual model, however, is confounded by the presence of a 5-cm-thick storm deposit layer present in boxcores collected immediately after the storm and bbl model output that contradicts the altimeter observations. The bbl model indicates that ripples continued to decrease in height and steepness from mid-day on 15 September through 18 September as near-bottom conditions became more energetic. A more reasonable explanation for these inconsistencies is that the seabed altimeter was detecting a highly concentrated layer of suspended sediments over the seabed due to the high estimated shear velocities at this time. On the 16th, when the seabed altimeter began to show the large fluctuations and elevated seabed elevation, a simple calculation of the critical shear velocity for full suspension using the predicted shear velocities shows that the threshold had been exceeded for all grain sizes less than or equal to 0.03 cm, which is over 50% of the volume of surface sediment found at the site based on grain-size analysis from surface samples. Further, calculations using the shear velocities that existed during peak storm conditions show that all grain sizes of 0.047 cm (approximately 90% of sediments at the site) would have been in full suspension. The grain-size analysis of the suspended sediments collected in the sediment trap corroborates the shear velocities predicted by the model and indicates that all sediments at the site

were suspended during peak conditions having a d_{90} value of 0.0663 cm. These data and calculations support the bbl model predictions, which indicated that ripple heights and steepness would have been decreasing and approaching wash out during peak storm conditions. Further, the presence of a highly concentrated layer of suspended sediment is corroborated by the ABS measurements which yielded very high returns in the lowest two bins above the seabed from 16–17 September. These measurements are in agreement with the model concentration profiles that showed very high concentrations of suspended sediments in the bottom 10 cm, which was approximately equal to the thickness of the wave boundary layer (calculated using model shear velocities) at this time (Figs. 7a, 8a).

The presence of a highly concentrated layer of suspended sediment is further supported by anecdotal diver reports. The existence of an oscillating suspended sediment layer (of lesser magnitude) immediately above the seabed has previously been observed by divers at the site during long-period swells from distant hurricane passages to the east of the study site. Thus, multiple lines of evidence exist that suggest the presence of a highly concentrated suspended sediment layer in the bottom boundary layer. The existence of such a layer easily accounts for the large discrepancy between the bbl model output and the seabed altimetry data and indicates that the seabed altimeter was not detecting the bottom during the height of the storm.

Assuming, then, that the seafloor altimetry data collected during peak storm conditions were measuring an artificially elevated seabed due to high concentrations of suspended sediments, it is conceivable that a 5-cm-thick storm *deposit* layer could be preserved even if there was a net decrease in seabed elevation of 2 cm. One plausible scenario emerges when the seabed altimetry data, boxcore data, and suspended sediment transport direction in the vicinity of the study area are simultaneously considered over the duration of the storm. Rather than accretion, the seafloor underwent maximum erosion during peak conditions when the transport was towards the southwest. At this time, the seabed altimeter was actually detecting high concentrations of suspended sediments, and therefore largely unable to record the 5 cm of reworking indicated by the thickness of the disturbed layer present in the cores. Given the turbulent mixing processes in the boundary layer during peak storm conditions causing inherent fluctuations in concentrations, the concentration of material within the near-bottom suspended sediment layer was not steady. Thus, during periods of relatively lower suspended sediment concentrations, the seabed altimeter was able to detect the seabed. Once such incident occurred at 1000 UTC on 18 September when a large decrease in seabed elevation is evident for one of the beams. This decrease in the altimetry data suggests a lowering of the seabed of approximately 5 cm from the previous burst to a level that is approximately equal to the elevation of the bottom of the observed storm deposit layer in the boxcore. At 1600 UTC, another beam appears to have successfully detected the seabed at a similar elevation. These data, coupled with net transport to the southwest and a limited availability of sediments northeast of the site, suggest that a period of intense, local erosion was occurring during peak storm conditions. Subsequently, when bottom conditions became less energetic and the coarser fraction of the suspended sands settled, all three beams were able to detect the seabed again, which was 2 cm below the pre-storm elevation. Given the various measured data available, the oxidized layer is inferred to represent the storm layer. However, due to the lack of an identifiable storm lag or sediment size-grading consistent with model outputs, this relationship is speculative. When both the thickness of the storm deposit layer and the pre- and post-storm bed elevations are accounted for, there was approximately 7 cm of storm reworking at the site (Fig. 10).

6. Conclusions

Sediment transport occurred on the mid-shelf over a 4.5-day period due to the close passage of Hurricane Isabel. The Styles and Glenn (2000) bottom boundary layer model used in this study appears to reasonably predict mean velocity profiles in the bottom boundary layer during storm conditions based on the comparisons between measured and modeled current profiles. The bbl model was used to quantify sediment transport during the event and indicated that suspended sediment transport was the dominant transport mode for the fine sediments throughout the event as shear velocities for full suspension were exceeded two days before the passage of the storm. The net direction of suspended sediment flux associated with the hurricane was to the southwest and shoreward. The suspended sediment transport that occurred during this event was an order of magnitude larger than the suspended sediment transport that occurred at the site during a moderate nor'easter storm in year 2000 (Wren and Leonard, 2002).

The presence of high levels of suspended sediments within the wave boundary layer caused the 1.5 MHz seabed altimeter to not detect the bottom during periods of large swell-dominated bottom conditions. The bbl model estimated that ripples on the seabed gradually decreased as the storm advanced towards the site, and full suspension conditions were approached during the peak storm conditions. Boxcores in conjunction with seabed altimetry data indicate that the seabed was reworked 7 cm by the physical processes that occurred

at the mid-shelf site throughout the 4.5-day duration of the passage of Hurricane Isabel.

Acknowledgements

The authors would like to thank Dr. Fred Bingham for making the ADCP data available for this study. We also thank Jay Souza, David Wells, and Morgan Bailey for their technical and diving support. We thank the captain and crew of the R/V *Cape Fear*. The authors also appreciate the comments from two anonymous reviewers. This manuscript was prepared by the authors under award number NA16RP2675 to the University of North Carolina at Wilmington from the National Oceanic and Atmospheric Administration, U.S. Department of Commerce.

References

Battisto, G.M., 2000. Field measurement of mixed grain size suspension in the nearshore under waves. M.S. Thesis. Virginia Institute of Marine Science, Glouster Point, VA.

Head, M.E., 2004. Use of high-resolution sidescan sonar data to quantitatively map and monitor a mid-continental shelf hard-bottom: 23 mile site Onslow Bay, North Carolina. M.S. Thesis. University of North Carolina at Wilmington, Wilmington, NC.

Li, M.Z., Amos, C.L., 1999. Field observations of bedforms and sediment transport thresholds of fine sand under combined waves and currents. Marine Geology 158, 147–160.

Madsen, O.S., 1995. Spectral wave–current bottom boundary layer flows. Proceedings of the 24th ICCE, vol. 1. ASCE, pp. 384–398.

Madsen, O.S., Wright, L.D., Boon, J.D., Chisholm, T.A., 1993. Wind stress, bed roughness and sediment suspension on the inner shelf during an extreme storm event. Continental Shelf Research 13, 1303–1324.

Madsen, O.S., Wikramanayake, P.N., 1991. Simple models for turbulent wave and current boundary layer flow. Contract Report, DRP 91-1. U.S. Army Corps of Engineers Research Center, Vicksburg, MS, 150 pp.

Meyer-Peter, E., Muller, R., 1948. Formulas for bed-load transport. Report on the Second Meeting of International Association for Hydraulic Research, pp. 39–64.

National Oceanographic Data Center, 2000. NOAA Coastal-Marine Automated Network Station FPSN7. http://www.ndbc.noaa.gov/FPSN7.

Nielsen, P., 1992. Coastal Bottom Boundary Layers and Sediment Transport. World Scientific Publishing, Singapore, 324 pp.

Ogston, A.S., Sternberg, R.W., 1999. Sediment-transport events on the northern California continental shelf. Marine Geology 154, 69–82.

Pietrafesa, L.J., Janowitz, G.S., Wittman, P.A., 1985. Physical oceanographic processes in the Carolina Capes. Oceanography of the Southeastern U.S. Continental Shelf, pp. 23–32.

Pietrafesa, L.J., Morrison, J.M., McCann, M.P., Churchill, J., Boehm, E., Houghton, R.W., 1994. Water mass linkages between the Middle and South Atlantic Bights. Deep-Sea Research II 41, 365–389.

Renaud, P.E., Riggs, S.R., Ambrose Jr., W.G., Schmid, K., Snyder, S.W., 1997. Biological–geological interactions: storm effects on macro-algal communities mediated by sediment characteristics and distribution. Continental Shelf Research 17 (1), 37–56.

Riggs, S.R., Ambrose Jr., W.G., Cook, J.W., Snyder, S.W., 1998. Sediment production on sediment-starved continental margins: the interrelationship between hard bottoms, sedimentological and benthic community processes, and storm dynamics. Journal of Sedimentary Research Section A: Sedimentary Petrology and Processes 68 (1), 135–148.

Styles, R., Glenn, S.M., 2002. Modeling bottom roughness in the presence of wave-generated ripples. Journal of Geophysical Research 107, 1–15.

Styles, R., Glenn, S.M., 2000. Modeling stratified wave and current bottom boundary layers on the continental shelf. Journal of Geophysical Research 105, 24119–24139.

Swart, D.H., 1974. Offshore Sediment Transport and Equilibrium Beach Profiles. Publication No. 131, Delft Hydraulics Lab, Delft, Netherlands.

Traykovski, P., Hay, A., Irish, J.D., Lynch, J.F., 1999. Geometry, migration, and evolution of wave orbital ripples at LEO-15. Journal of Geophysical Research 104, 1505–1524.

Wiberg, P.L., Harris, C.K., 1994. Ripple geometry in wave dominated environments. Journal of Geophysical Research 99 (C4), 775–789.

Wiberg, P.L., Drake, D.E., Harris, C.K., Noble, M., 2002. Sediment transport on the Palos Verdes shelf over seasonal to decadal time scales. Continental Shelf Research 22, 987–1004.

Williams, J.J., Rose, C.P., 2001. Measured and predicted rates of sediment transport in storm conditions. Marine Geology 179, 121–133.

Wright, L.D., Xu, J.P., Madsen, O.S., 1994. Across-shelf benthic transports on the inner shelf of the Middle Atlantic bight during the ''Halloween storm'' of 1991. Marine Geology 118, 61–71.

Wright, L.D., Boon, J.D., Green, M.O., List, J.H., 1986. Response of the mid-shoreface of the southern mid-Atlantic bight to a 'North-easter'. Geo-Marine Letters 6, 153–160.

Wren, P.A., Leonard, Lynn A., 2002. Physical processes and sediment transport in Onslow Bay, NC. Eos Transactions AGU 83 (47) (Fall Meet. Suppl., F690).